Photomodulation of the proton affinity and acid gated photochromism of a novel dimethylaminophenyl thiazole diarylethene

Y. Kutsunugi[a], C. Coudret[b,*], J.C. Micheau[b], T. Kawai[a]

[a] Graduate School of Materials Science, NAIST, 8916-5 Takayama, Ikoma, Nara 630-0192, Japan
[b] Université de Toulouse, UPS, IMRCP, 118 route de Narbonne, F-31062 Toulouse Cedex 9, France

ARTICLE INFO

ABSTRACT

The acid-gated photochromism and the photomodulation of fluorescence and proton affinity of a novel dimethylaminophenyl thiazole diarylethene in MeCN were investigated from a kinetic point of view. Photomodulation of the proton affinities has been estimated from acid titrations and numerical modelling of the acid induced T-photochromism. The basicities of the thiazole and dimethylamino protonation sites are different by only one pK unit. Upon ring- closure, their relative proton affinities are reversed. Our investigations underline the role of the thiazole protonation in the carbon-carbon bond weakening of the closed form and validate the role of the proton as catalyst in the gated T-photochromism.

1. Introduction

The development of photoswitchable molecular devices is encompassing very different fields, from the design of photo-responsive systems able to regulate a chemical reaction to physical applications in optical memory media with non-destructive readout capability. These two issues are basically related to the following questions: (i) how the photoisomerisation process affects its hosting medium? (ii) How the medium affects the photochromic response? From a more basic point of view, these two concepts are related to the so-called photomodulation and gated-photochromism. To date, most of the responsive dyes are constructed as bifunctional molecules involving a photochromic unit connected to a stimuli sensitive moiety. If the difference between the physico-chemical properties of the two isomers of a photochromic molecule is sufficient to change the macroscopic behaviour of a bulk medium, it is said that this compound exhibits a performance of photomodulation. For instance, Feringa et al. have shown that the fluorescence and chirality of photoswitchable inherently dissymmetric *cis* and *trans* alkenes can be reversibly photomodulated [1]. Moreover, since the first report

concerned with the photoregulation of catalytic activity has been published by Ueno et al. [2] during the hydrolysis of *p*-nitrophenyl acetate catalysed by β-cyclodextrin in presence of a photo-isomerisable *cis*–*trans* *p*-(phenylazo) benzoate, many other examples of the photoswitching of catalytic activity have been published [3]. They are described in a review by Hecht et al. [4].

With the aim to lock the photochromic unit into a specific isomer -especially towards light- a related phenomenon has been explored: the gated-photochromism where the photoisomerisation reactivity is made sensitive to some external stimuli such as reactive chemicals. One of the first attempts to observe gated-photochromism was reported by Irie et al. [5]. The effect is based on the inhibition of the photochromic reactivity of a diarylethene when the molecule adopts a parallel conformation. This conformation was stabilised by the presence of suitably disposed interlocking arms. The molecule regains photoactivity when the intramolecular lock is released by the addition of hydrogen bond breaking or reducing agents. Another example of gated photochromism is achieved by controlling either the conformation or intra-molecular proton transfer of diary-lethenes by using intra or inter molecular hydrogen bonds [6]. More recently, it has been shown that the incorporation of acid-base sensitive groups in diarylethenes might lead to multi-state molecular switches *i.e.* to acid-gated photochromism [7].

The relationships between photomodulation and gated photo-chromism are illustrated on Scheme 1 in the particular case of a pH

* Corresponding author.
E-mail addresses: tkawai@ms.naist.jp (Y. Kutsunugi), coudret@chimie.ups-tlse.fr (C. Coudret).
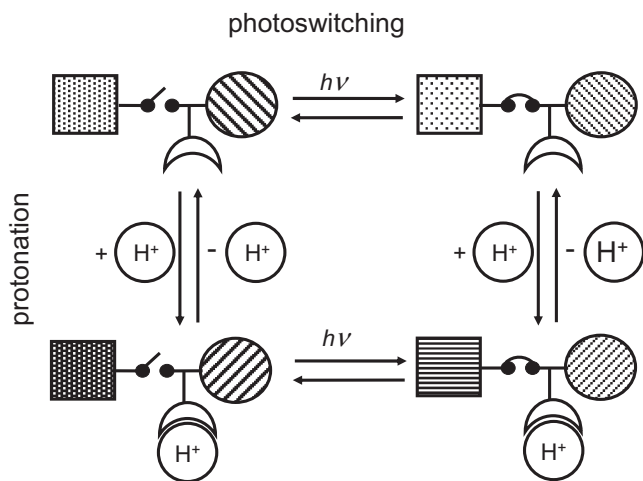
photoswitching

Scheme 1.

sensitive photochromic molecule [8]. All the necessary processes construct a square network. The two horizontal processes, related to the photoswitching between open and closed forms, lead to the gating of the photochromic property (coloration or discoloration) as the photoswitching process is made sensitive to protonation. The two vertical processes involve "dark processes" and compare the two isomer's affinity for proton. Thus, along this point of view, one can change this constant with light, thus "photomodulating" the protonation equilibrium.

Several families of photochromic molecules can be used to develop gated-photochromism and photomodulation phenomena. Among them, spiropyranes and spirooxazines bearing crown-ethers have been synthesised for analytical chemistry purposes [9]. However, to increase the photochromic performance and the fatigue resistance, it appears that looking towards the diarylethene (DTE) family [10] could be more profitable. Indeed, the open and closed isomers of photochromic diarylethenes have not only different absorption UV/visible spectra but also many different physical and chemical properties. For instance, the switching of luminescence [11] and the photomodulation of ionic interactions and reactivity [12] are some properties closely related to the photomodulation or gated-photochromism that have been rather well documented. However, in more details, it must be pointed-out that the most notorious papers in this domain are focused on only one of the two quantitative aspects, either on photomodulation or on gated-photochromism. For instance, Odo et al. [13] have shown that a pK_a switching can be induced by the change in a π-conjugated system based on photochromism, but the possible variations of the quantum yields under the influence of pH variations have not been explored. Another example can be found in the Yumoto et al. [14] paper about the control of the photoreactivity of some diarylethene derivatives by quaternarization of a pyridylethynyl group, but the probable changes of pK's according to the isomeric state open or closed have not been scrutinised. Because photomodulation and gated-photochromism are intimately related, it must be borne in mind that the two processes are occurring simultaneously. This detail could be of importance, especially when aiming towards potential practical applications. To the best of our knowledge this is only in the paper by Lehn et al. [15] that the two concepts ("*photochemical pK_a-modulation and gated photochromic properties*") are investigated simultaneously.

In order to afford a new example where photomodulation and gated-photochromism are investigated simultaneously we have submitted a novel pH-sensitive diarylethene to irradiation and

pH variations, recorded the UV/visible spectra, and build a comprehensive model based on a square network as in Scheme 1. The specificity of our approach is that all species and all processes are considered simultaneously under realistic conditions. The details of the used numerical technique can be found in a free access website [16]. Curve fitting allows the assessment of several relatively inaccessible parameters such as quantum yields, multiple-equilibria stability constants or kinetic rate constants.

2. Experimental

2.1. Products

2.1.1. 4-(Dimethylamino)benzothioamide

To a slurry of 70% sodium hydrosulfide hydrate (0.92 g = 10 mmol) and magnesium chloride hexahydrate (1.02 g = 5 mmol) in DMF (10 mL) was added 4-(dimethylamino)benzonitrile (0.73 g = 5 mmol) in one portion, and the mixture was stirred at room temperature for 2 h. The resulting green slurry was poured into 20 mL of water, stirred for 20 min in 1 N HCl, then filtered and washed with water to give pure compound by yellow solid. Yield 80%, ^{1}H NMR (300 MHz, Acetone-d_6): δ 8.48 (br, NH$_2$) 8.01 (d, 2H), 7.48 (d, 2H), 3.03 (s, 6H).

2.1.2. 4,5-Bis(2-methylbenzo[b]thiophen-3-yl)-2-(4-(trifluoromethyl)phenyl)thiazole (**1o**)

2-hydroxy-1,2-bis(2′-methylbenzo[b]thiophen-3′-yl)ethanone (1.76 g = 5 mmol) was added to a solution of 4-(dimethylamino)benzothioamide (0.65 g, 3.2 mmol) in trifluoroacetic acid (3.0 ml) and the mixture was kept for 24 h at room temperature, diluted with diethyl ether, and neutralised with aqueous solution of sodium hydroxide. The aqueous phase was extracted with diethyl ether, the extracts were washed in succession with water, and 20% solution of sodium hydroxide, and water again, dried over MgSO$_4$, and evaporated. Yield 1.0 g (40%). ^{1}H NMR (300 MHz, DMSO-d_6) d 7.90−7.88(m, 4H), 7.69(br, 2H), 7.30−7.26(m, 4H), 6.83(d, 2H), 3.02(s, 6H), 2.02(s, 6H) ppm. HRMS(EI) calcd. for C$_{29}$H$_{24}$N$_2$S$_3$ (M$^+$) 496.1102, found (M$^+$) 496.1100.

2.1.3. Solvent and reactants

MeCN for spectroscopy, anhydrous trifluoroacetic acid and aqueous solution (70% acid) of HClO$_4$ were of the highest purity available. They were used as purchased.

2.2. Data recording and analysis

2.2.1. Photochromism

Absorption spectra of the MeCN solutions of compound **1** (8×10^{-6} mol L^{-1}) were recorded on an HP 8451 diode array spectrophotometer. The photochemical irradiation was derived from a 200 W, IR filtered, high pressure mercury lamp equipped with single-line interference filters and high transmission optical fibre. The photochemical reactor was a 1 cm × 1 cm quartz cell (1 cm optical path) containing 2.5 cm^3 of solution. The optical fibre was fitted tightly at the neck of the cell. The monochromatic light intensity was determined directly in the stirred reactor using an acidic aqueous solution of potassium ferrioxalate ($I_0^{313} = (2 \pm 0.4) \times 10^{-6}$; $I_0^{365} = (4 \pm 0.9) \times 10^{-6}$ mol L^{-1} s^{-1}). The thermosted solution (25 °C) was stirred with a magnetic stirrer bar. Absorption maximum and irradiation wavelengths were monitored simultaneously until a PSS was reached. The kinetic modelling technique of the Abs *vs* time traces using the home made "sa" software has been already described [17].

2.2.2. Protonation

0.08 mol L^{-1} MeCN solutions of TFA or $HClO_4$ were added step-by-step to a 8×10^{-6} mol L^{-1} solution of **1** in a 1 cm × 1 cm quartz cell using a microliter syringe. Ratio of concentrations at 10^4 insured that the volume increase after 1000 equivalents of acid added was only +10%.

2.2.3. Establishment of a model

Table 1 displays the list of processes occurring in the assumed model, where **1o** represents the neutral open form, **1oH$^+$** the mono-protonated open form, **1oH$_2^{2+}$** the di-protonated open form, **1c** the neutral closed form, **1cH$^+$** the mono-protonated closed form and **1cH$_2^{2+}$** the unstable di-protonated closed form. This model is the simplest possible taking into account all the qualitative experimental observations. It is based on the same ideas than the square network displayed in Scheme 1. Moreover, to increase the chemical realism, according to Kolthoff et al. [18], the formation of hydrated protons and water homoconjugates in MeCN has been taken into account when using the partially hydrated strong perchloric acid solution (molar ratio $H_2O:HClO_4 = 1:2.4$). The corresponding formation constants of the water homoconjugates have been gathered from the literature. The others have been adjusted by the model from the fitting of various Absorbance *vs* acid added and Absorbance *vs* time experimental curves.

With trifluoroacetic acid (TFA), only processes 9 and 10 have been considered replacing H^+ by TFA and **1oH$^+$** species by a loose [**1o**.TFA] ion-pair. From the simultaneous fitting of the variations of the absorbance at 360 and 428 nm as a function of the number of equivalents of acid added, k_9 has been estimated at 425 ± 20 $M^{-1}s^{-1}$ using $k_{10} = 1$ s^{-1}.

With perchloric acid ($HClO_4$) which has been assumed to be fully dissociated, the second protonation occurs and k_9 and k_{11} have been estimated at respectively 4×10^4 and 4×10^3 $M^{-1}s^{-1}$ using $k_{10} = k_{12} = 1$.

2.2.4. Spectral recalculations

They are based on the Beer's law: $Abs(\lambda) = \Sigma_i \varepsilon_{xi}(\lambda)^*[X]_i$, where $Abs(\lambda)$ is the recorded UV/visible spectrum of the mixture of compounds X_i (in absorbance units), $\varepsilon_{xi}(\lambda)$ is the UV/visible spectrum of the compound X_i in L mol^{-1} cm^{-1} units and $[X]_i$ the concentration of compound X_i in mol L^{-1} units. The concentrations of the species $[X]_i$ are given by the model. $\varepsilon_{xi}(\lambda)$ are the solutions of a system of linear equations.

2.2.5. Thermal bleaching

Colored solutions were obtained by irradiating a 3.5×10^{-5} M MeCN solution of **1** until a photostationary state (PSS) was reached (OD_{max} *ca* 0.37). Then, the appropriate amount of $HClO_4$ was added. UV–vis. kinetics traces of the absorbance at 552 nm (λ_{max} of the protonated closed form) were then acquired at 25 °C. The whole model including processes 1–17 has been used for kinetic data analysis. Previously determined first and second protonation equilibrium constants of the open form have been fixed while mono- and di-protonation affinities and thermal kinetic rate of ring-opening of the closed form have been adjusted to fit the thermal bleaching kinetics.

3. Results and discussion

Recently, thiazole containing DTE-like molecules, such as angular terarylenes, have been developed for fast thermal bleaching rate purposes [19]. The presence of the heterocyclic nitrogen atom makes the molecule sensitive to Lewis acidic cations. Thus, the stability of the closed form of a triphenylangular terthiazole was found to be considerably affected by the presence of protonation sites [20]. In the present paper, we investigate the photochromism in neutral and acidified MeCN of a new dimethylaminophenyl thiazole diarylethene [21]. The presence of two protonation sites on the dimethylamino group and on the thiazole ring makes the compound **1** a strong candidate for proton gated-photochromism and pK_a photomodulation experiments. The key step of the synthesis is the construction of the central thiazole ring via the condensation of a symmetrical acyloin with a thioamide. For comparison purpose a derived ammonium salt was also prepared by room temperature methylation of the dimethylamino group of compound **1** (Fig. 1).

Table 1
Processes 1 to 8 are devoted to the description of the formation of water homoconjugates. They allow a correction of the acid concentrations. Processes 9 to 17 depict the first and second protonation of the open and closed form and the acid catalysed ring-opening. Reverse rate constants have been put arbitrarily at 1 in order to insure that the establishment of the various equilibria are sufficiently rapid. In these conditions, the equilibrium constant is expressed by the same value than the direct rate constant of the corresponding forward process.

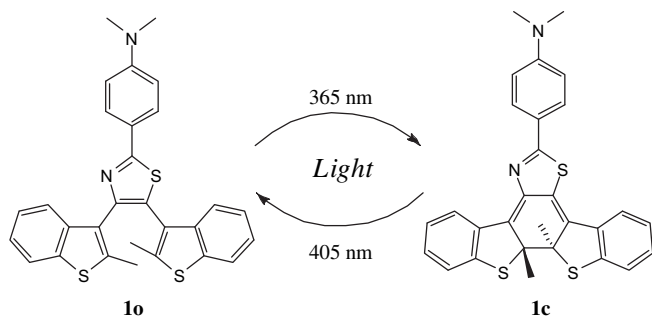| n°	List of processes	Rate of process	Rate constant of process
1	$H^+ + H_2O \rightarrow H_3O^+$	$k_1[H][H_2O]$	$k_1 = 1.4 \times 10^2$
2	$H_3O^+ \rightarrow H^+ + H_2O$	$k_2[H_3O^+]$	$k_2 = 1$
3	$H_3O^+ + H_2O \rightarrow H_5O_2^+$	$k_3[H_3O^+][H_2O]$	$k_3 = 2.7 \times 10^3$
4	$H_5O_2^+ \rightarrow H_3O^+ + H_2O$	$k_4[H_5O_2^+]$	$k_4 = 1$
5	$H_5O_2^+ + H_2O \rightarrow H_7O_3^+$	$k_5[H_5O_2^+][H_2O]$	$k_5 = 3.3 \times 10^4$
6	$H_7O_3^+ \rightarrow H_5O_2^+ + H_2O$	$k_6[H_7O_3^+]$	$k_6 = 1$
7	$H_7O_3^+ + H_2O \rightarrow H_9O_4^+$	$k_7[H_7O_3^+][H_2O]$	$k_7 = 1.2 \times 10^4$
8	$H_9O_4^+ \rightarrow H_7O_3^+ + H_2O$	$k_8[H_9O_4^+]$	$k_8 = 1$
9	$\mathbf{1o} + H^+ \rightarrow \mathbf{1oH^+}$	$k_9[\mathbf{1o}][H^+]$	$k_9 = $ see text
10	$\mathbf{1oH^+} \rightarrow \mathbf{1o} + H^+$	$k_{10}[\mathbf{1oH^+}]$	$k_{10} = 1$
11	$\mathbf{1oH^+} + H^+ \rightarrow \mathbf{1oH_2^{2+}}$	$k_{11}[\mathbf{1oH^+}][H^+]$	$k_{11} = 4ex10^3$ $M^{-1}s^{-1}$
12	$\mathbf{1oH_2^{2+}} \rightarrow \mathbf{1oH^+} + H^+$	$k_{12}[\mathbf{1oH_2^{2+}}]$	$k_{12} = 1$
13	$\mathbf{1c} + H^+ \rightarrow \mathbf{1cH^+}$	$k_{13}[\mathbf{1c}][H^+]$	$k_{13} = 10^3$ $M^{-1}s^{-1}$
14	$\mathbf{1cH^+} \rightarrow \mathbf{1c} + H^+$	$k_{14}[\mathbf{1cH^+}]$	$k_{14} = 1$
15	$\mathbf{1cH^+} + H^+ \rightarrow \mathbf{1cH_2^{2+}}$	$k_{15}[\mathbf{1cH^+}][H^+]$	$k_{15} = 10^4$ $M^{-1}s^{-1}$
16	$\mathbf{1cH_2^{2+}} \rightarrow \mathbf{1cH^+} + H^+$	$k_{16}[\mathbf{1cH_2^{2+}}]$	$k_{16} = 1$
17	$\mathbf{1cH_2^{2+}} \rightarrow \mathbf{1oH_2^{2+}}$	$k_{17}[\mathbf{1cH_2^{2+}}]$	$k_{17} = (1.5 \pm 0.1) \times 10^{-1}$ s^{-1}
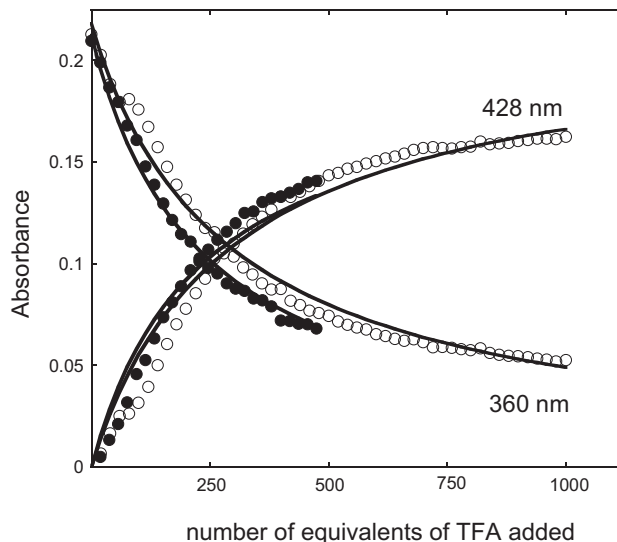
Fig. 1. Variations of the absorbance monitored at two selected wavelengths during the addition of TFA in a MeCN solution of **1o**; ([**1o**]$_0 = 7.7 \times 10^{-6}$ M). Two independent experiments are displayed (filled circles and open circles). Dots are the experimental data points, solid lines are the simulations by the model.

Scheme 2.

Fig. 3. Determination of the quantum yields of photocoloration ($\Phi_{oc} = 0.52$) and photobleaching ($\Phi_{co} = 0.27$) from the kinetic modelling of the Absorbance vs time curves recorded under continuous monochromatic irradiation for photocoloration at 365 nm (black dots) and at 405 nm for photobleaching (open squares). ([**1o**] + [**1c**]) = 4.8×10^{-5} mol L^{-1} in neutral MeCN solution. At PSS(365), [**1c**]/[**1o**] = 3.1, at PSS(405), [**1c**]/[**1o**] = 0.05.

3.1. Photochromism

In neutral MeCN, compound **1** exhibits the expected P-photochromism of the diarylethene (DAE) series, i.e. photocoloration under UV irradiation and photobleaching under visible light (Scheme 2).

In order to determine the quantum yields of photocoloration and photobleaching together with the UV/visible absorption spectrum of the closed form, a photokinetic analysis of the absorbance vs time kinetic curves recorded under continuous monochromatic irradiation has been carried-out. Under 365 nm UV irradiation, the system slowly evolves until a photosteady state (PSS) at which the rate of photocoloration is exactly counterbalanced by the rate of photobleaching (Fig. 2). The presence of a clear-cut isosbestic point is a strong indication that only two isomers are present and that there is no photodegradation.

By combining photocoloration and photobleaching records, it is possible using a simple P-photochromism model (**1o**← → **1c** $h\nu$; $h\nu$) to find out the two quantum yields of photocoloration (Φ_{oc}) and photobleaching (Φ_{co}) without the need of a time- and product-consuming chemical isolation of the closed isomer (Fig. 3). The modelling also delivers the conversion rate ([**1c**]/[**1o**]) which has been achieved at the PSS. Therefore the whole UV/visible spectrum of the closed isomer **1c** can be estimated (see below).
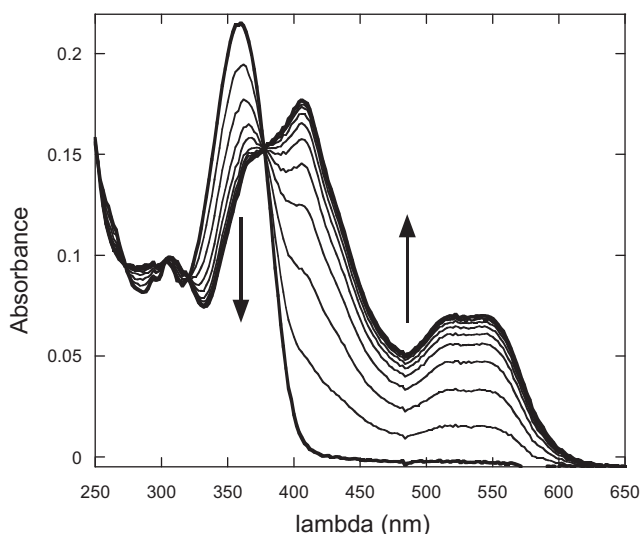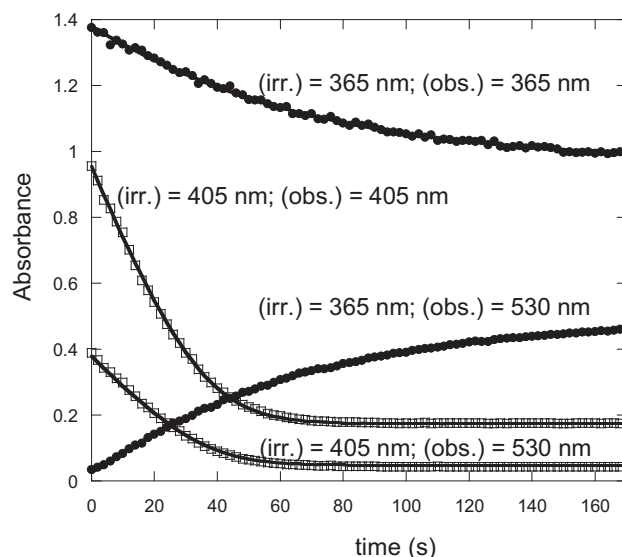
The kinetic analysis also delivers the PSS conversion rate ($\approx 76\%$ of closed form under 365 nm irradiation) and consequently the molar absorption coefficient of the closed isomer **1c** at the observation wavelength (530 nm) can be estimated at 13,200 L mol^{-1} cm^{-1}.

3.2. Fluorescence

When excited at 360 nm in MeCN, the open form **1o** exhibits a strong fluorescence peaking at ca. 440 nm (Fig. 4). The large Stokes shift (≈ 80 nm) suggests the presence of a twisted intermolecular charge transfer (TICT) excited state.
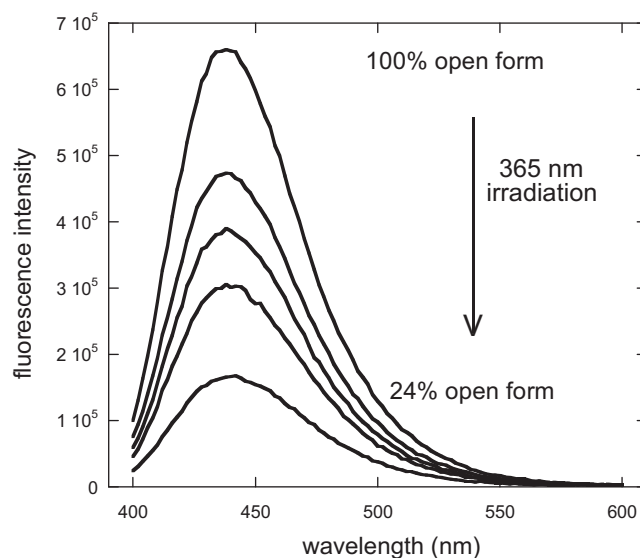

Fig. 2. Photocoloration of compound **1o** ([**1o**]$_0$ = 7.7×10^{-6} M) under 365 nm irradiation in MeCN. Note the formation of the closed form absorbing at 410 and 530 nm (wide band) with an isosbestic point at 380 nm. The concentrations of the closed form at the PSS is: [**1c**]$_{PSS}$ = 5.8×10^{-6} M.
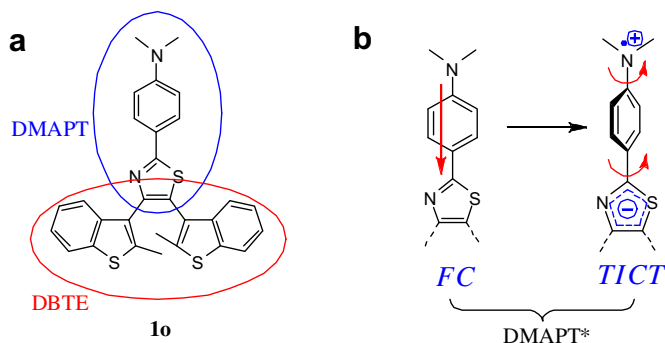

Fig. 4. Decay of the fluorescence of the open form during the photocoloration process **1o** → **1c** under 365 nm irradiation. The residual fluorescence at the 365 nm PSS is 24% of the initial signal.

Scheme 3.

It is indeed clear from the structure of compound **1o** that the central moiety, the 2-(p-dimethylaminophenyl)thiazole DMAPT shows the classic push-pull system, with the N,N-p-dimethylaminophenyl as the donor group and the thiazol-2-yl as the acceptor one (Scheme 3a). This chromophore is very close to the one studied by Dey et al. [22], namely the 2-(p-dimethylaminophenyl)benzothiazole DMAPBT. The main low energy band in the DMAPBT absorption spectrum was attributed to the charge transfer transition between the electron donating dimethylamino group and the electron withdrawing benzothiazolyl one: it is indeed solvatochromic with a λ_{max} in MeCN of ca 355 nm that equates nicely the main transition of the open form **1o**. Thus, **1o** is a bichromophoric system, with a DMAPT unit fused to a dibenzothienylethene (DBTE) photochromic one (Scheme 3a). The DMAPT-localised excited state would then adopt two extreme conformations, a planar "Franck-Condon" (FC) one, with the geometry of the ground state, and a relaxed twisted one (TICT) in which the charges are fully separated, and responsible of the long wavelength emission (Scheme 3b).

Upon continuous irradiation, the fluorescence signal decays in a parallel way to the photoisomerisation process. These results confirm that the conversion rate at the 365 nm PSS is $\approx 76\%$ of the closed form, a value identical to that obtained from the kinetic modelling displayed on Fig. 3. These data also indicate that the closed isomer **1c** is not contributing to the total fluorescence spectrum. A very rough energetic scheme can be proposed (Scheme 4) for both situations: in the open state, the molecule's Franck Condon planar excited state can relax either by the photocyclization of the DBTE part or by luminescence via a TICT intermediate. In the closed state the DBTEc unit is acting as an

intramolecular non luminescent quencher of the DMAPT's excited states (either FC or TICT).

3.3. Acidochromism

A very nice bathochromic spectral shift is observed upon acid addition in a MeCN solution of the open form **1o**. It is interesting to remark that trifluoroacetic (TFA) and perchloric (HClO₄) acid give rise to the same phenomenon. However, this occurs not for the same amount of equivalents. Typically, it needs about 1000 equivalents of TFA to reach a maximum, while only less than 5 are sufficient for HClO₄.

A determination of the association constants between **1o** and acid has been performed from the numerical modelling of the variation of the absorbance during the incremental addition of acid equivalents using a simple $A + B \leftarrow \rightarrow C$ model:

For TFA addition : $\mathbf{1o} + TFA \leftarrow \rightarrow [\mathbf{1o}.TFA]$ K_{1oTFA}

[**1o**.TFA] is a loose ion-pair where the proton is closer to **1o** than to TFA.

For HClO₄ addition : $\mathbf{1o} + H^+ \leftarrow \rightarrow \left[\mathbf{1}.H^+\right]$ K_{1oH}

HClO₄ is assumed to be fully dissociated.

This model allows the determination of the association constants of the open form **1o** with TFA, K_{1oTFA} at around 425 ± 25 M^{-1} and with H$^+$, $K_{1oH} \approx 4 \times 10^{+4}$ M^{-1}. The result with TFA deserves to be compared with a recent NMR determination of the TFA association constant with a terthiazole photochromic derivative [23] (≈ 27 M^{-1}) where the association is occurring at the thiazole rings.

In the case of compound **1o**, it is not easy to say where the first protonation takes place. Dey et al. [22] have studied the influence of protonation of the absorption spectrum of the DMAPBT chromophore. This investigation is interesting, because of the presence of basic nitrogen atoms on both electron donating and withdrawing groups. Thus, if the protonation occurs on the thiazole moiety enhancing its electron withdrawing ability, one expects a lowering of the charge transfer energy. On the other hand, protonation of the dimethylamino group should destroy its electron donating ability thus moving the transition to higher energy. A similar result is also assumed for the twice protonated species. This leads us to assign the protonation sites of compound **1o** from the spectral changes of the DMAPT chromophore's main transition. The bathochromic spectral shift observed on Fig. 5 would be indicative that the first protonation of the open form **1o** is occurring on the thiazole
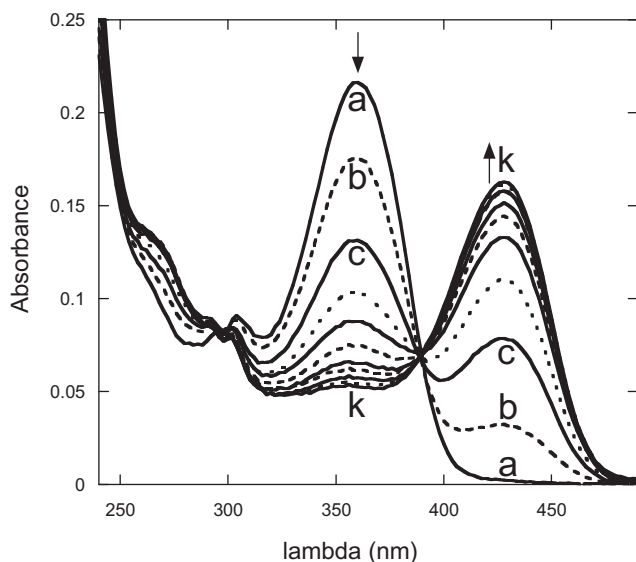

Scheme 4.

843
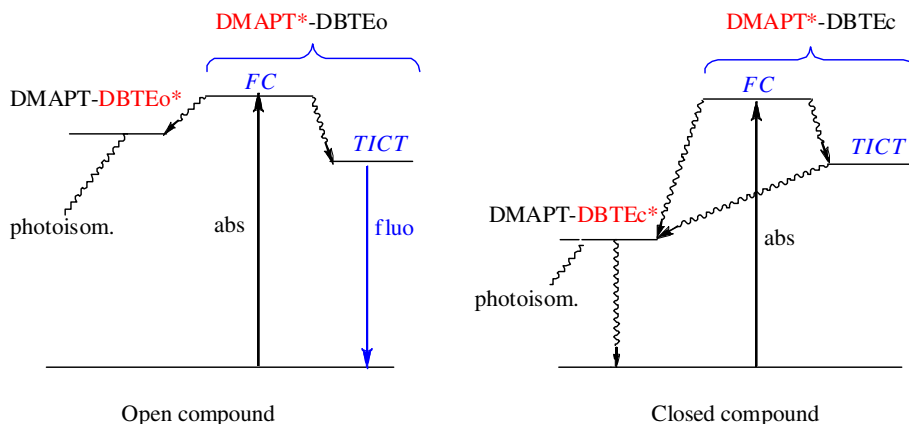
Fig. 5. Spectral variation during the addition of TFA on **1o** in anhydrous MeCN. a: [**1o**] $= 8 \times 10^{-6}$ M; [TFA] $= 0$; b: [TFA] $= 8 \times 10^{-4}$ M (100equivalents); c $= 200$eq.; k: 1000 equivalents, [TFA] $= 8 \times 10^{-3}$ M. Note the bathochromic shift from 360 nm to 428 nm. Isobestic point at 390 nm indicates that **1o** and [**1o**.TFA] are the only absorbing species.

heterocycle. Moreover, as displayed on Fig. 6, the step-by-step addition of only some equivalents of HClO$_4$ is sufficient to observe a gradual bleach of the 428 nm band and the appearance of a new blue shifted absorption at 290 nm. This observation is consistent with what should be expected if the second protonation of **1o** occurs on the dimethylamino group [24]. The spectral shift is completed after the addition of less than 300 equivalents of HClO$_4$ and the process is fully reversible. The 428 nm band is recovered then converted into the initial 360 nm band during the neutralisation of the HClO$_4$ in excess by the addition of the corresponding amount of triethylamine.

It is remarkable that whatever the acid used (TFA or HClO$_4$) the intermediate "monoprotonated" spectrum is preserved. This
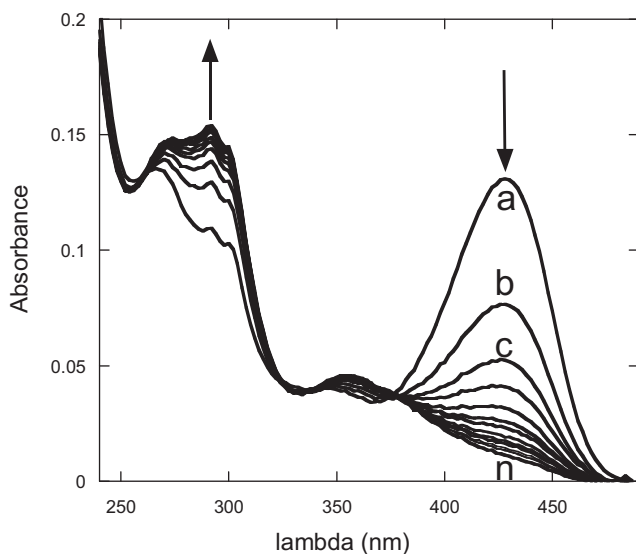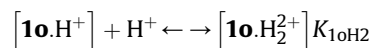
should imply that the ion pair between the trifluoroacetate and the **1o**H$^+$ cation should be loose or more or less dissociated.

The spectral variations in presence of an excess of HClO$_4$ have been analysed by considering the second protonation. This was done by taking into account a second equilibrium:

$$\left[\mathbf{1o}.H^+\right] + H^+ \longleftrightarrow \left[\mathbf{1o}.H_2^{2+}\right] K_{1oH2}$$

allowing the estimation of a second association constant $K_{1oH2} \approx 4 \times 10^{+3}$ M^{-1} *i.e.* one order of magnitude lower than for the first protonation. This result confirms the presence of two protonation sites.

It is not simple to compare the values of these association constants with some pK_a values found in the literature. The first reason stays in the structural differences between compound **1** and the closest parent molecule, namely the DMAPBT (dimethyl aminophenyl benzothiazole). The second is related to the solvent used, pure water *vs* MeCN/water mixture. Nevertheless, if we consider the values published by Dey et al. [22] for the monocation and the dication of DMAPBT at respectively 2.9 and 0.3 in water, it is possible to estimate their corresponding values in MeCN by adding *ca* 3pK units [25]. Finally, the recalculation of the proton affinity constants from the corrected pK_a lead to two results not too far from the expected order of magnitude, namely 8×10^5 M^{-1} for the mono- protonation and to 500 M^{-1} for the di-cation formation.

The UV spectra of the mono- and di-protonated species have also been recalculated from the species distribution delivered by the model (Fig. 7).

Fig. 8 displays the recalculated UV/visible spectra of the neutral closed form (b). Spectrum c shows the shifted spectrum of the closed form in presence of aqueous perchloric acid.

As for the open form, the spectra of both closed forms (b and c) are dominated by a sharp absorption in the blue–UV region that is likely to come from the central *p*-dimethylaminophenyl thioimidate moiety (note that the thiazole aromatic ring does not exist in the ring-closed form). Again, applying the same analysis as Dey et al. can help in the protonation site assignment. Indeed, the main transition in **1c** is hypsochromically shifted in presence of free protons. Consequently it is likely that the mono-protonation of **1c** occurs on the dimethylamino group. The basicity locus inversion of

Fig. 6. Gradual decrease of the 428 nm band during the step-by-step addition of an excess of HClO$_4$ in a 8×10^{-6} M solution of **1o**. a: 20; b: 40; c: 60; n: 280 equivalents added. Note the increase of the absorption at 292 nm.
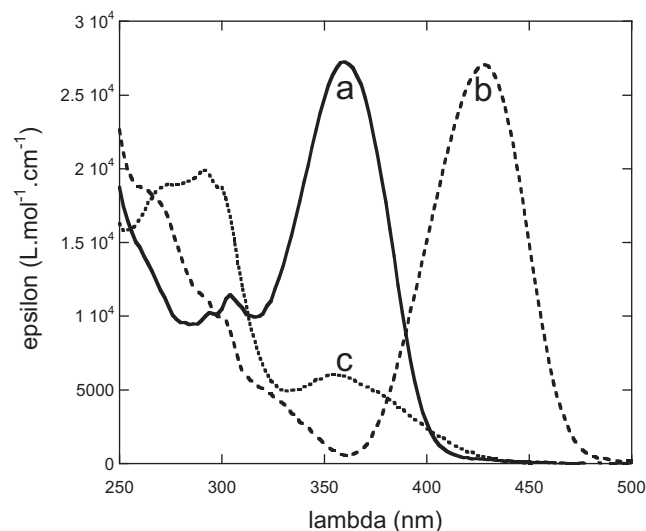

Fig. 7. UV/visible spectrum of the free open form (a); recalculated spectrum of the mono-protonated open form (b) and of the di-protonated open form (c). The spectrum of the ion-pair with TFA is identical to (b).
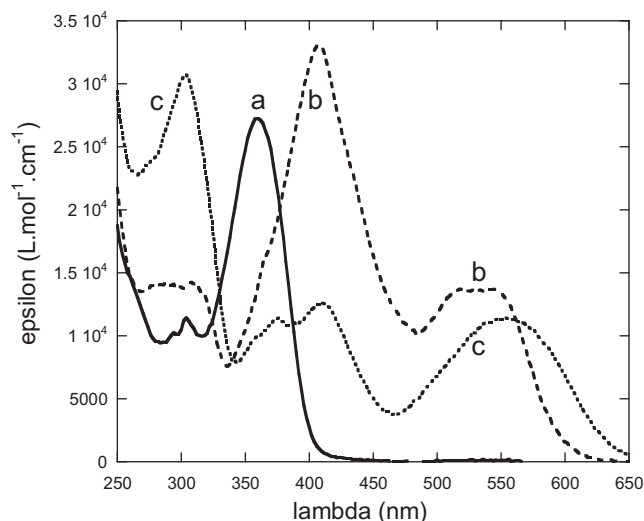
Fig. 8. UV/visible spectra of the neutral closed form b. c: shifted spectrum of the closed form in strongly acidic solution. For the sake of comparison, the spectrum of the neutral open form is labelled: a.

the first protonation which takes place on the thiazole in the open form and on the dimethylamino in the closed form has to be related to the photochromic reaction that affects the thiazole ring. Another spectral change concerns the long wavelength transition at ca 500 nm. It is then likely that the slight tailing in the red and the simplification of the band's envelope could be due to a charge effect coming from the protonation [26].

3.4. Acid catalysed T-photochromism

Under aqueous $HClO_4$ addition, there is a rapid variation of the spectrum of the closed form as depicted on Fig. 9.

After few seconds, the closed form **1c** exhibits the same UV/visible spectrum as with TFA. This result is an indication that a protonation (like the loose ion-pair) is taking place at the
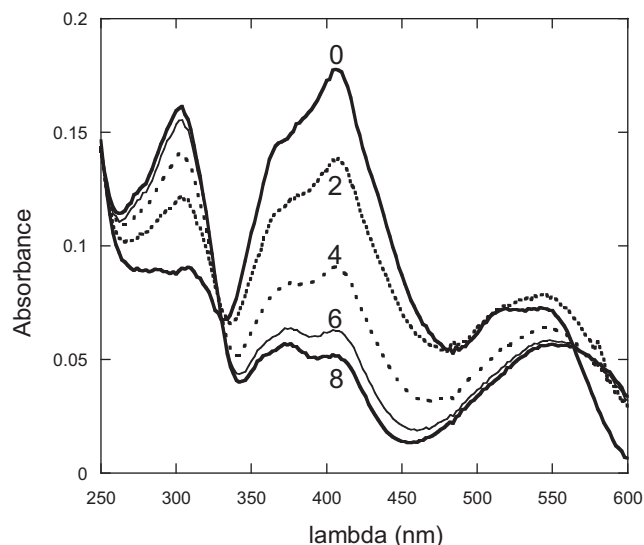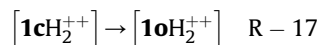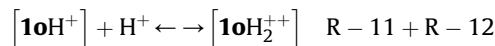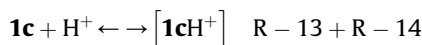
dimethylamino site. Moreover, in strong acidic conditions, this spectrum is no longer stable and undergoes a slow thermal bleaching (Fig. 10). The second protonation of the closed form concerns the heterocyclic imino nitrogen of the former thiazole ring. Since no UV–vis spectrum can be extracted for this twice protonated species, the latter must evolve quickly into the open form. This mechanistic scheme is analogous to what was observed on a parent terthiazole photochromic compound [19,21].

The rate of ring opening depends on the amount of acid added. For low $HClO_4$ concentrations, the rate of bleaching is roughly proportional to the amount of acid added. On the contrary, when the acid concentration is sufficiently high, a saturation phenomenon (the rate no longer increases) occurs and the kinetic traces are superposed (Fig. 11).

The following kinetic scheme with kinetic equations numbering according to Table 1 has been used to describe the acid catalysed thermal bleaching of **1**.

$$\mathbf{1c} + H^+ \leftarrow \rightarrow \left[\mathbf{1cH^+} \right] \quad R-13+R-14$$

$$\left[\mathbf{1cH^+} \right] + H^+ \leftarrow \rightarrow \left[\mathbf{1cH_2^{++}} \right] \quad R-15+R-16$$

$$\mathbf{1o} + H^+ \leftarrow \rightarrow \left[\mathbf{1oH^+} \right] \quad R-9+R-10$$

$$\left[\mathbf{1oH^+} \right] + H^+ \leftarrow \rightarrow \left[\mathbf{1oH_2^{++}} \right] \quad R-11+R-12$$

$$\left[\mathbf{1cH_2^{++}} \right] \rightarrow \left[\mathbf{1oH_2^{++}} \right] \quad R-17$$

The model considers the simultaneous mono- and di-protonation of both the closed and open form. It is assumed that the set of rapid equilibria are continuously displaced under the influence of the irreversible ring opening process. This situation is similar to the hydration of the flavylium ion as described by Mc Clelland et al. [27] where multiple equilibria are displaced by a coupling with an irreversible reaction. With such a model fitted with the appropriate parameters *i.e.* the already estimated proton affinities of the open form **1o**, it is possible to approximately reproduce a set of four

Fig. 9. Rapid variation (from 0 to 8 s) of the UV/visible spectrum of the closed form after $HClO_4$ addition in MeCN and vigourous shaking. $[\mathbf{1c}]_0 = 5 \times 10^{-6}$ M; $[HClO_4]_0 = 2.5 \times 10^{-3}$ M. Note the red-shift of the closed form spectrum with solvent change. Spectrum 8 is no longer stable and undergoes a slow bleaching.
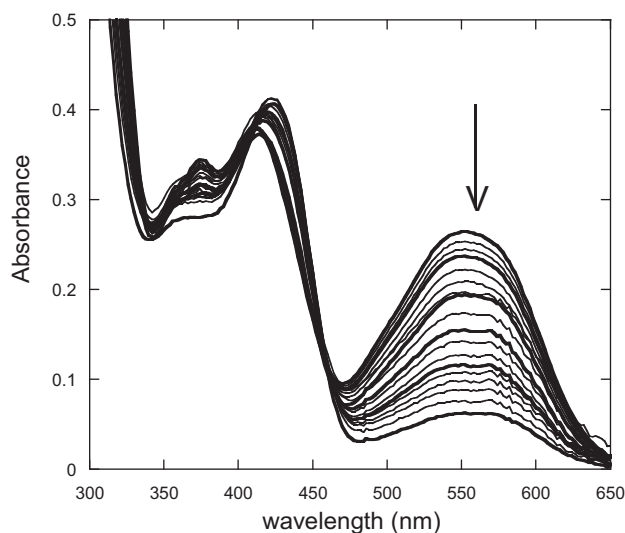

Fig. 10. Acid catalysed thermal bleaching of the closed form, $[\mathbf{1c}]_0 = 2 \times 10^{-5}$ M. Changes in Δt are indicated by bold solid line spectra $\Delta t = 600$ s, then 1200, then 1800, 2400 and 3000 s. $[HClO_4]$ added $= 4 \times 10^{-3}$ M.
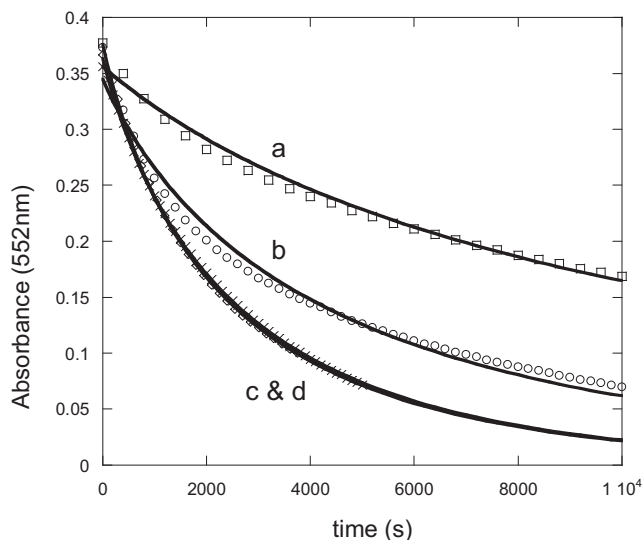
Fig. 11. Kinetic records of the thermal bleaching of the closed form **1c** (3×10^{-5} mol L^{-1}) under strong acidic conditions: [HClO$_4$] = 4.2×10^{-3} M(a); 7×10^{-3} M (b); 1.05×10^{-2} M (c); 1.4×10^{-2} M (d). Dots are experimental data points; solid lines: simulation by the model. Note that the model reproduces quite well the superposition of the two kinetic curves (c and d) recorded at the higher acid concentrations. The slight departures seen on curves a and b could be attributed to some model imperfections or experimental bias.

kinetic traces recorded at variable initial acid concentrations. The ability of the model to reproduce the traces superposition (saturation effect) at the higher acid concentration must be pointed-out. Such a feature is an argument for the global validation of the model although it cannot be excluded that some missing processes could occur. Within the framework of these hypothesis, the model allows the estimation of the mono ($\approx 10^{+3}$ M^{-1}) and di- ($\approx 10^{+4}$ M^{-1}) protonation constants of the closed form and the first-order thermal ring opening rate constant ($k_{\text{opening}} = 1.5 \pm 0.5 \times 10^{-1}$ s^{-1}).

3.5. Analysis of the gated-photochromism and photomodulation

Results gathered in Table 2 show that compound **1** displays a gated-photochromism effect under mild and strong acid conditions. On one hand, spectral shifts around 70–100 nm are observed on the absorption spectra of the open and closed isomers. On the other hand, the photocoloration/photobleaching quantum yields ratio is decreased by a factor of more than 2 in mild acidic medium. It is likely that protonation could change the excited state deactivation and evolution paths. Moreover, strong acid triggers the ring-opening of the otherwise stable closed form **1c**. Fig. 4 also illustrates the photomodulation of the fluorescence of compound **1o**. The open form **1o** is fluorescent while the closed form **1c** is not.

Moreover, thanks to the numerical modelling of the acid induced T-photochromism, photomodulation of the proton affinities has also been observed (Table 3). Although there is only one order of magnitude difference between the stability constants of

Table 2
Gated-photochromism of **1**. The quantum yields of photocoloration and photobleaching in mild acidic conditions have been determined in the presence of 1000 equivalents of TFA. Strong acidic conditions are attained with HClO$_4$.

	$\lambda_{\max}$ (open) (nm)	$\varepsilon_{\max}$ (open)	$\lambda_{\max}$ (closed) (nm)	$\varepsilon_{\max}$ (closed)	Φ_{AB}	Φ_{BA}
Neutral	360	27,300	530; 405	13,200	0.52	0.27
Acid (mild)	428	27,200	552; 305	10,700	0.32	0.39
Acid (strong)	292	20,000	Not stable	Not stable	–	–

Table 3
Photomodulation of the proton affinity constants.

Compound **1**	Mono- protonation	Di-protonation
Open **1o**	$4 \times 10^{+4}$ M^{-1}	$4 \times 10^{+3}$ M^{-1}
Closed **1c**	10^{+3} M^{-1}	10^{+4} M^{-1}

the mono- and di-cation, their ratio depend on the open **1o** or closed **1c** state of the isomer under consideration.

Open and closed isomers behave in a reverse way. For the open isomer, the dication formation is less easy than the mono. On the contrary, for the closed form, there is a cooperative effect, the di-protonation is easier. For the open form **1o**, the mono-protonation site is then assumed to be at the thiazole ring with the higher stability constant and the second at the dimethylamino site with the lower constant. The situation for the closed form **1c** is different, di-protonated species are kinetically unstable, therefore the only protonated species is the mono-protonated one where protonation is occurring at the dimethyl-amino site. Consequently, the attack of the second proton is taking place on the thiazole moiety. This second protonation is expected to give rise to a weakening of the ring-closing bond as it was already suggested in the acid triggered terthiazole T-photochromism [19]. It is possible that this affinity change could be related to a proton swap between the two basic sites during the photoswitch of the monoprotonated species.

4. Conclusion

Compound **1** exhibits the required features to display some gated-photochromism and photomodulation properties, namely the presence of a photochromic DAE-like kernel associated with two basic sites of different proton affinities.

From the point of view of gated-photochromism, several effects deserve to be pointed-out. There are clear-cut spectral shifts of both the open and closed form under protonation. Quantum yields of both photocoloration and photobleaching are sensitive to the presence of TFA. When compound **1** is mono-protonated, its quantum yield of photocoloration is decreased by about 40%, while its quantum yield of photobleaching increases by about the same amount. It is liable that this effect originates from a specific reactivity of the excited states either at the level of the deactivations or avoided crossing paths. The last point to be mentioned is the transformation of a typical DAE-like P-photochromism into a variable T-photochromism under the influence of HClO$_4$ addition. A mechanism including the lack of stability of the di-protonated closed form has been developed and it has been shown that it is able to reproduce rather accurately the effect of HClO$_4$ initial concentration.

Our approach was based on numerical modelling and multi-experiment curve fitting. This specific technique was applied to handle either equilibrium (titration) or time dependent (kinetic traces) data. We have been able to estimate the photomodulation of the proton affinity. Ring-closure increases the proton affinity of the heterocyclic nitrogen. This last point is remarkable because a similar phenomenon of basicity increase in the photochromic kernel has already been observed in a previous P- to T-photochromism switch with a terthiazole compound.

From this analysis, it appears that many photochromic molecules bearing ion-affinity sites or reactive fragments are relevant to the gated-photochromism or photomodulation concept. Their quantitative studies are not easy because all these effects are coupled and cannot be isolated without difficulties. However, by combining careful spectroscopic titration or kinetic monitoring with numerical data analysis it could be possible to reach some

parameters with a sufficient accuracy to reveal the most interesting systems and to direct the synthesis of the next generation of molecules. Ion-sensing appears as a reachable practical application of gated-photochromism/photomodulation [28].

References

[1] Huck NPM, Feringa BL. Dual-mode photoswitching of luminescence. J Chem Soc Chem Commun; 1995:1095–6.
[2] Ueno A, Takahashi K, Osa T. Photoregulation of catalytic activity of beta-cyclodextrin by an azo-inhibitor. J Chem Soc Chem Commun; 1980:837–8.
[3] Cacciapaglia R, Di Stefano S, Mandolini L. The bis-barium complex of a butterfly crown ether as a phototunable supramolecular catalyst. J Am Chem Soc 2003;125:2224–7.
[4] Stoll RS, Hecht S. Artificial light-gated catalyst systems. Angew Chem Int Ed 2010;49:5054–75.
[5] (a) Irie M, Miyatake O, Uchida K. Blocked photochromism of diarylethenes. J Am Chem Soc 1992;114:8715–6;
(b) Irie M, Miyatake O, Uchida K, Eriguchi T. Photochromic diarylethenes with intralocking arms. J Am Chem Soc 1994;116:9894–900.
[6] (a) Takeshita M, Choi CN, Masahiro Irie M. Enhancement of the photo-cyclization quantum yield of 2,2′-dimethyl-3,3′-(perfluorocyclopentene-1,2-diyl)bis(benzo[b]-thiophene-6-sulfonate) by inclusion in a cyclodextrin cavity. Chem Commun; 1997:2265–6;
(b) Ohsumi M, Fukaminato T, Irie M. Chemical control of the photochromic reactivity of diarylethene derivatives. Chem Commun; 2005:3921–3.
[7] Chen ZH, Zhao SM, Li ZY, Zhang Z, Zhang FS. Acid/alkali gated photochromism of two diarylperfluorocyclopentenes. Sci China Ser B Chem 2007;50:581–6.
[8] Yokoyama Y, Yamane T, Kurita Y. Photochromism of a Protonated 5-dimethylamino-indolylfulgide: a Model of a Non-destructive Readout for a Photon Mode Optical Memory. J Chem Soc Chem Commun; 1991:1722–4.
[9] Kimura K, Nakahara Y. Analytical and separation chemistry by taking advantage of organic photochromism combined with macrocyclic. Chem Anal Sci 2009;25:9–20.
[10] Irie M. Diarylethenes for memories and switches. Chem Rev 2000;100:1685–716.
[11] Yam VVW, Ko CC, Zhu NY. Photochromic and luminescence switching properties of a versatile diarylethene-containing 1,10-phenanthroline ligand and its rhenium(I) complex. J Am Chem Soc 2004;126:12734–5.
[12] Nakashima T, Goto M, Kawai S, Kawai T. Photomodulation of ionic interaction and reactivity: reversible photoconversion between imidazolium and imidazolinium. J Am Chem Soc 2008;130:14570–5.
[13] Odo Y, Matsuda K, Irie M. pKa switching induced by the change in the pi-conjugated system based on photochromism. Chem Eur J 2006;12:4283–8.
[14] Yumoto K, Masahiro Irie M, Matsuda K. Control of the photoreactivity of diarylethene derivatives by quaternarization of the pyridylethynyl group. Org Lett 2008;10:2051–4.
[15] Kawai SH, Gilat SL, Lehn JM. Photochemical p Ka-modulation and gated photochromic properties of a novel diarylethene switch. Eur J Org Chem; 1999:2359–66.
[16] For a chemical kinetics tutorial and "sa" software downloading, the reader is invited to visit the web site: http://pagesperso-orange.fr/cinet.chim/index.html.
[17] Metelitsa AV, Lokshin V, Micheau JC, Samat A, Guglielmetti R, Minkin VI. Photochromism and solvatochromism of push–pull or pull–push spiroindolinenaphthoxazines. Phys Chem Chem Phys 2002;4:4340–5.
[18] Kolthoff IM, Chantooni Jr MK. Protonation in acetonitrile of water, alcohols, and diethyl ether. J Am Chem Soc 1968;90:3320–6.
[19] Kawai S, Nakashima T, Atsumi K, Sakai T, Harigai M, Imamoto Y, Kamikubo H, Kataoka M, Kawai T. Novel photochromic molecules based on 4,5-dithienyl thiazole with fast thermal bleaching rate. Chem Mater 2007;19:3479–83.
[20] Coudret C, Nakagawa T, Kawai T, Micheau JC. Weak acid triggers the ring-opening of an otherwise long-lived triangle terthiazole closed isomer. New J Chem 2009;33:1386–92.
[21] Kutsunugi Y, Kawai S, Nakashima T, Kawai T. Photochromic properties of terarylene derivatives having a pi-conjugation unit on central aromatic ring. New J Chem 2009;33:1368–73.
[22] Dey J, Dogra SK. Dual fluorescence of 2-(4′- (N, N-dimethy1amino)phenyl) benzothiazole and its benzimidazole analogue: effect of solvent and pH on electronic spectra. J Phys Chem 1994;98:3638–44.
[23] Nagakawa T, Serpentini CL, Coudret C, Micheau JC, Kawai T. Substrate induced catalysis: deciphering the weak acid triggered bleaching of an angular ter-thiazole photochromic dye. Dyes Pigments 2011;89:271–7.
[24] Another robust argument to confirm that the second protonation of the open form is taking place at the dimethyl amine site is the similarity between the spectra of $1oH_2^{2+}$ and its N-methylammonium derivative (data not shown).
[25] Garrido G, Rosés M, Ràfols C, Bosch E. Acidity of several anilinium derivatives in pure tetrahydrofuran. J Soln Chem 2008;37:689–700.
[26] These conclusions are confirmed by the close match between the UV/visible spectra of the acidified closed form and its N-methylammonium derivative. The mono-protonation of the closed form is occurring at the anilinium site.
[27] McClelland RA, Gedge S. Hydration of the flavylium ion. J Am Chem Soc 1980;102:5838–48.
[28] Zhou ZG, Xiao S, Xu J, Liu Z, Shi M, Li F, Yi T, Huang C. Modulation of the photochromic property in an organoboron-based diarylethene by a fluoride ion. Org Lett 2006;8:3911–4.